Rutkowska, M.; Duda, M.; Macina, D.; Górecka, S.; Debek, R.; Moreno-Rodríguez, JM.; Díaz Morales, UM.... (2019). Mesoporous Beta zeolite functionalisation with FexCry oligocations; catalytic activity in the NH3-SCO process. Microporous and Mesoporous Materials. 278:1-13. https://doi.org/10.1016/j.micromeso.2018.11.003

Functionalization of mesoporous Beta zeolite with Fe_xCr_y oligocations and examination of its activity in NH_3-SCO process

M. Rutkowska[1*], M. Duda[1], D. Macina[1], S. Górecka[1], R. Dębek[2], U. Díaz[3], L. Chmielarz[1]

[1]Jagiellonian University, Faculty of Chemistry, Ingardena 3, 30-060 Kraków, Poland

[2]AGH University of Science and Technology, Faculty of Energy and Fuels, Department of Fuels Technology, al. A. Mickiewicza 30, Kraków, Poland

[3]Instituto de Tecnología Química, UPV-CSIC, Universidad Politécnica de Valencia, Avenida de los Naranjos, s/n, 46022 Valencia, Spain

[*]Corresponding author. Tel.: +48 126632096, fax: +48 126340515. E-mail address: rutkowsm@chemia.uj.edu.pl (M. Rutkowska)

Keywords: Beta zeolite, mesoporous Beta, oligocations, iron, chromium, ammonia oxidation, NH_3-SCO

Abstract

In the presented studies H-Beta zeolite and H-Beta/meso (mesoporous Beta zeolite obtained by mesotemplate-free method) were modified with Fe3, Fe2Cr, FeCr2 and Cr3 oligocations by ion-exchange method (for the comparison also modification with Fe isolated cations was done). Successful synthesis of mesoporous Beta zeolite was confirmed by several techniques such as N_2-sorption, XRD, AAS or NH_3-TPD. Modified porosity and acidity of Beta zeolite, as well as the used source of metals, influenced the form (coordination and aggregation), content and reducibility of Fe- and Cr-species in the samples (UV-vis-DRS, AAS, H_2-TPR). The obtained samples were tested as catalysts in the process of selective catalytic oxidation of

ammonia to dinitrogen (NH_3-SCO). The highest activity and selectivity to nitrogen was obtained for the bimetallic Fe-Cr samples obtained by deposition of suitable oligocations.

1. Introduction

Ammonia (NH_3) is one of the most significant N-containing gaseous pollutants [1-2]. For many decades it is used as a reactant or is produced as a by-product in various industrial processes (e.g. nitric acid and nitrogen fertilizer production plants, urea manufacturing or $DeNO_x$ process) [e.g. 1, 3-8]. Therefore, due to environmental concerns, the reduction of ammonia concentration in the emitted waste streams is incessantly important.

Different methods of NH_3 elimination were proposed [1-2, 4-5]. Among them, selective catalytic oxidation (SCO) of ammonia to dinitrogen and water vapour is one of the most promising method for the removal of NH_3 from flue gases containing oxygen [e.g. 1-9]. In this process nitrogen oxides (N_2O and NO) are the main by-products. The effective SCO catalyst should operate in a relatively low temperature range (180-400°C) in order to reduce the operational costs connected with additional heating of waste streams [1, 7-11]. Moreover, it should selectively direct the reaction to the formation of the main products and should also be stable in the presence of water vapour or other typical components of flue gases such as CO_x and SO_x [1, 12].

Various types of materials have been reported in the literature as catalysts for the NH_3-SCO process. They can be classified into three groups – noble metals (e.g. Pt, Pd, Ru, Rh, Ir, Ag [e.g. 1-2, 5-6, 9-10]), transition metal oxides (e.g. CuO, Fe_2O_3, MnO_2, Co_3O_4 [1-2, 5-10]) and catalysts based on zeolites (e.g. ZSM-5 modified with copper and iron [1-2, 5-6, 9-10]). Noble metals are very active in ammonia oxidation in the low temperature region [1-2, 5, 7, 9]. However, high price and relatively low selectivity to N_2 are the main drawbacks of such catalysts [1-2, 6, 9]. On the other side transition metal oxides are characterized by higher

selectivity to dinitrogen in comparison to noble metals, but they are significantly less active at lower temperatures [e.g. 1-2, 5-6, 9].

The last group of catalysts for selective catalytic oxidation of ammonia, which is based on zeolites, presents many advantages for the catalytic purposes, such as uniform crystalline structure, high surface area, ion-exchange properties, shape selectivity, or controlled concentration and strength of acid sites [1, 13]. Various types of zeolites modified with transition metals were reported in the scientific literature as highly active, selective and relatively cheap catalysts of the NH_3-SCO process [2, 6, 9]. Among them, especially Y, ZSM-5 and Beta zeolites modified with Fe, Cu, Cr or Mn were widely studied as potential catalysts for the oxidation of ammonia and showed promising results [e.g. 2, 14-18]. Long and Yang [14] found the following trend of the catalytic activity of ZSM-5 modified with transition metals in the NH_3-SCO process: Fe > Cu > Cr > Pd > Mn > Ni ≈ Co. Additionally, it was reported that a decrease in the Si/Al improves the catalytic performance of zeolites in the oxidation of ammonia [6].

It should be mentioned that the catalytic system characterized by very high activity (close to 100% conversion of ammonia) and selectivity to nitrogen as well as very good stability in a long term at low temperatures (<400°C) was still not found [2]. Therefore, continuous studies and development of new types of the oxidation catalysts are still very important.

Zeolite Beta, which is characterized by larger pores diameter in comparison to ZSM-5, could facilitate the transport of the gaseous reactants to the active sites and improve the overall effectiveness of many catalytic processes [2]. On the other hand, in many papers it was shown that iron and chromium present very high activity in the NH_3-SCO process [e.g. 1, 9, 14, 19]. Recently, Macina et al. [19] studied catalytic activity of iron and chromium aggregates ($[M_3O(OAc)_6 \cdot AcOH \cdot 2H_2O]NO_3$) deposited on the surface of mesoporous silicas (SBA-15 and HMS). It was reported that the catalytic performance of the synthesized materials strongly

depend on the composition of deposited transition metal oligocations and significantly better activity showed the samples doped with bimetallic oligocations (Cr_2Fe_1 or Cr_1Fe_2) in comparison to the mesoporous silica modified with monometallic species (Cr_3 or Fe_3) [19].

The modification of microporous zeolites with oligocations (triple-metallic aggregates) can be facilitated by the generation of micro-mesoporous structure. One of the possible effective methods of mesoporous Beta synthesis is mesotemplate-free method, which by the controlled aggregation of zeolite seeds enable one-pot synthesis of micro-mesoporous zeolites [13, 20]. Modification of the zeolite porous structure strongly influences the form (coordination and aggregation) of transition metals introduced by ion-exchange method, what is the crucial issue in the case of deposition of oligocations as precursors of catalytically active species. In our previous studies [13, 20-24] micro-mesoporous zeolites with BEA, MFI, CHA or MWW topologies, modified with Fe, Cu or Co showed high catalytic activity and stability in the process of N_2O decomposition as well as in the NH_3-SCO and NH_3-SCR processes.

Therefore, our research has been focused on the synthesis of catalysts for selective catalytic oxidation of ammonia, based on the conventional microporous Beta zeolite as well as mesoporous Beta zeolite (prepared by mesotemplate-free method) modified with Fe, Cr and Fe-Cr aggregates. The influence of textural and surface properties of the catalysts on the content and form of introduced metals and their catalytic performance in NH_3-SCO was investigated.

2. Experimental methods

2.1. *Catalysts preparation*

In the first step of the synthesis, suspension of Beta zeolite nanoparticles was obtained following the procedure described earlier in [13, 20]. Tetraethylammonium hydroxide (TEAOH, 35%, Sigma-Aldrich), which acts as a structure-directing agent, was mixed with

double distilled water and fumed silica (Aerosil 200, Evonic). Aqueous solution of $NaAlO_2$ (Sigma-Aldrich), prepared in a second batch, was added to the first mixture and stirred for 1 h. The resulting synthesis gel with the molar ratio of SiO_2 : 0.024 Al_2O_3 : 0.612 TEAOH : 0.200 HCl : 21 H_2O was divided into two parts which were separately transported into two autoclaves and aged at 150°C.

In the case of micro-mesoporous Beta zeolite, after 24 h of hydrothermal treatment at 150°C the milk-like suspension of Beta zeolite nanoparticles with the Si/Al molar ratio of 21was obtained. Than the first autoclave was cooled down and the suspension of nanoparticles was acidified with concentrated HCl with the proportion: 5 mL of acid per 18 mL of the nanoseeds slurry. Acidification in mesotempate-free method limits the aggregation and growth of the zeolite nanoparticles (inter-particle mesopores are created). The mixture after acidification was transported into the autoclave and hydrothermally treated at 150°C for 72 h. The obtained gel-like product was washed, dried and calcined at 600°C for 6 h.

To prepare conventional microporous Beta zeolite, hydrothermal treatment of the nanoparticles in the second autoclave was continued for 7 days. After aging the obtained solid product was filtered, washed, dried in ambient conditions and calcined at 600°C for 6 h.

The obtained samples were converted from Na- to H-form by triple ion-exchange with a solution of NH_4NO_3 (0.5 M, Sigma-Aldrich) at 80°C for 1h. Finally, the samples were washed, dried and calcined at 600°C for 6 h.

In the next step, the samples were modified with Cr-Fe oligocations of variable metal ratios using acetate salts of suitable oligocations. The acetate complexes, $[Cr_{3-x}Fe_xO(OAc)_6 \cdot AcOH \cdot 2H_2O]NO_3$ (where x = 0, 1, 2 or 3), were prepared according to the procedure presented in [19]. $Cr(NO_3)_3 \cdot 9H_2O$ (POCH) and $Fe(NO_3)_3 \cdot 9H_2O$ (POCH) were dissolved in a suitable proportion in anhydrous ethanol. Then acetic anhydride (POCH) was added dropwise and the mixture was cooled down in an ice bath (after heat evolution). The

obtained precipitates of the suitable acetate salts were filtered, dried at 60°C and denoted as Fe3, CrFe2, Cr2Fe and Cr3 (depending on the composition of triple-metallic aggregates).

Oligocations were introduced to conventional and micro-mesoporous Beta zeolites by classical ion-exchange with the proportion - 100 mL of the solution of suitable oligocations (total concentration of metals was 0.2 $g \cdot L^{-1}$) per 1 g of zeolite. Ion exchange was performed for 24 h at ambient temperature (three times for each sample). Then the samples were filtered, washed with distilled water and dried.

For the comparison the conventional and micro-mesoporous Beta zeolite were modified using an aqueous solution of $FeSO_4 \cdot 7H_2O$ (0.2 g of iron per 1 L, Sigma-Aldrich). To avoid oxidation of Fe^{2+} the ion-exchange process was performed under anaerobic conditions. Ion-exchange was repeated three times in these same conditions (24 h at ambient temperature, 100 mL of $FeSO_4$ solution per 1 g of zeolite).

Dried samples modified by ion-exchange with Fe-Cr oligocations or with a $FeSO_4$ solution were calcined at 600°C for 6 h. The sample codes of the final samples are presented in Tab. 1.

Tab. 1. Textural properties of the samples determined from the N_2-sorption measurements

Sample code	S_{BET} [m^2/g]	S_{EXT} [m^2/g]	V_{MIC} [cm^3/g]	V_{MES} [cm^3/g]
H-Beta	749	72	0.273	0.125
H-Beta/meso	620	323	0.120	0.894
Fe3-Beta	657	67	0.238	0.134
Fe3-Beta/meso	570	321	0.100	0.731
Fe2Cr-Beta	678	75	0.245	0.125
Fe2Cr-Beta/meso	576	315	0.107	0.824
FeCr2-Beta	715	74	0.259	0.141
FeCr2-Beta/meso	588	316	0.112	0.875
Cr3-Beta	719	90	0.256	0.145
Cr3-Beta/meso	606	335	0.111	0.898
Fe-Beta	689	77	0.247	0.131
Fe-Beta/meso	553	332	0.113	0.909

2.2. Catalysts characterization

Textural properties of the samples were determined by N_2 sorption at -196°C using a 3Flex v1.00 (Micromeritics) automated gas adsorption system. Prior to the analysis, the samples were degassed under vacuum at 350°C for 24 h. The specific surface area (S_{BET}) of the samples was determined using the BET (Braunauer-Emmett-Teller) model according to the recommendations of Rouquerol at al. [25]. The micropore volume and external surface area were calculated using the Harkins and Jura model (t-plot analysis, thickness range 0.55-0.85 nm). Mesopore volume was calculated from the desorption branch using the BJH model (Kruk-Jaroniec-Sayari empirical procedure) in the range of 1.7-30 nm. The pore size distributions were determined from the desorption branch of dinitrogen isotherm by applying density functional theory (DFT). For calculations model assuming dinitrogen adsorption in cylindrical pores was used.

The X-ray diffraction (XRD) patterns of the samples were recorded using a Bruker D2 Phaser diffractometer. The measurements were performed in the 2 theta range of 5 - 50° with a step of 0.02°.

Surface acidity (concentration and strength of acid sites) was studied by temperature-programmed desorption of ammonia (NH_3-TPD). The measurements were performed in a flow microreactor system equipped with QMS detector (Prevac). Prior to ammonia sorption, the samples were outgassed in a flow of pure helium at 600°C for 30 min. Subsequently, the microreactor was cooled to 70°C and the sample was saturated in a flow of gas mixture containing 1 vol.% of NH_3 diluted in helium for about 120 min. Then, the catalyst was purged in a helium flow until a constant base line level was attained. Desorption was carried out with a linear heating rate (10°C/min) in a flow of He (20 mL/min).

Transition metals content and Si/Al ratio were analysed by means of atomic absorption spectroscopy (Spectra AA 10 Plus, Varian).

The structure of the synthesized iron-chromium acetate complexes was studied by FTIR spectroscopy. The measurements were performed using a Nicolet 6700 FTIR spectrometer (Thermo Scientific) equipped with DRIFT accessory and MCT detector. The dried samples were grounded with dried potassium bromide powder (4 wt%) and the measurements were carried out in the wavenumber range of 800-2000 cm^{-1} with a resolution of 2 cm^{-1}.

UV-vis-DR spectroscopy was used to study the coordination and aggregation of iron and chromium species introduced into the obtained samples. The measurements were performed using an Evolution 600 (Thermo) spectrophotometer in the range of 200-900 nm with a resolution of 2 nm.

The reducibility of the samples was studied by temperature-programmed reduction with H_2 (H_2-TPR). Measurements were carried out in a flow system using thermal conductivity detector (VICI, Valco instruments). Before each experiment the sample (0.1 g) was outgassed in a flow of argon (20 mL/min) by its heating to 500°C with the rate of 15°C/min. The hydrogen uptake (5 vol.% of H_2 diluted in Ar, flow rate 20 mL/min) was analysed in the temperature range of 60-900°C (heating rate of 10°C/min).

2.3. Catalytic tests

Catalytic studies of NH_3-SCO were performed in a fixed-bed quartz microreactor. The experiments were done at atmospheric pressure and in the temperature range from 200 to 600°C. The reactant concentrations were continuously measured using a quadrupole mass spectrometer (Prevac) connected directly to the reactor outlet. For each experiment 0.1 g of catalyst (particles sizes in the range of 0.160-0.315 mm) was placed on quartz wool plug in the reactor and outgassed in a flow of pure helium at 600°C for 1 h. The gas mixture containing 5000 ppm of NH_3 and 25000 ppm of O_2 diluted in pure helium (total flow rate of 40 mL/min) was used.

3. Results and discussion

3.1. Parent conventional and micro-mesoporous Beta

Textural properties of conventional and micro-mesoporous Beta zeolites were investigated by low-temperature dinitrogen sorption measurements. Fig. 1A and B present dinitrogen sorption isotherms and pore size distribution of the parent samples respectively. The shape of H-Beta isotherm characteristic of microporous zeolites (type I(a)), changed in the case of micro-mesoporous sample and shows hysteresis loop characteristic of mesoporous materials (isotherm of type IVa). The hysteresis loop (type H4) observed in the case of H-Beta/meso proved the creation of aggregated zeolite crystals with the interparticle mesopores in the wide range of sizes [26]. DFT pore size distribution presented in Fig. 1B confirmed the presence of mesopores in H-Beta/meso in the range of pore sizes between 12-37 nm. The generation of mesoporosity occurred in a favour of the reduced microporosity, especially < 1 nm. Analysing the textural parameters for H-Beta and H-Beta/meso (Tab. 1), leads to the conclusion that application of mesotemplate-free method resulted in material with reduced micropore volume (more than 2 times) and significant development of the external surface area (increased about 4.5 times) as well as volume of mesopores (increased about 6 times). Thus, the relative increase in mesoporosity was higher than the relative decrease in microporosity, what clearly shows that the modification of textural properties of Beta zeolite by mesotemplate-free method was successful.

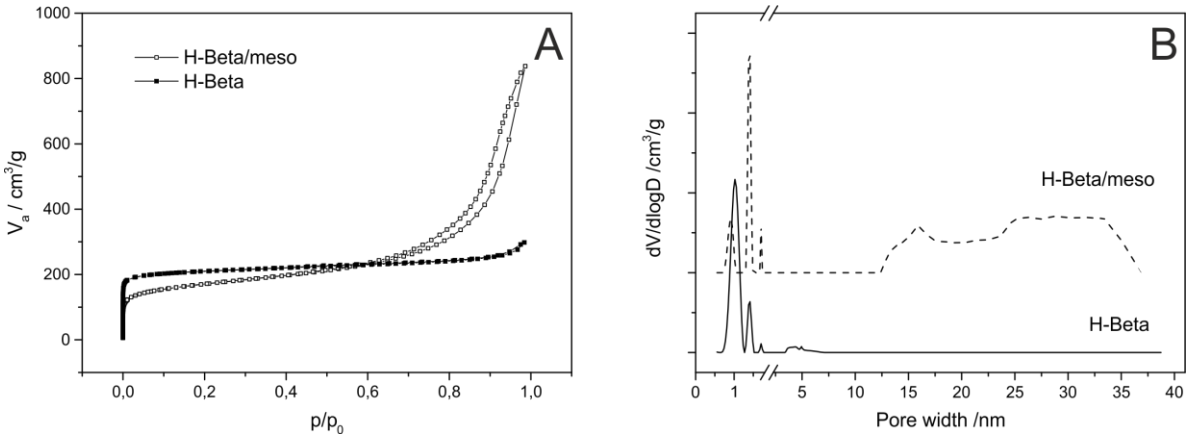

Fig. 1. Nitrogen adsorption-desorption isotherms (A) and pore size distribution (B) of the parent H-Beta and H-Beta/meso samples

The crystalline nature of H-Beta/meso obtained by mesotemplate-free method was investigated by XRD technique (Fig. 2A). The intensity of the reflections obtained for micro-mesoporous sample was slightly lower in comparison to conventional H-Beta zeolite. However, the difference between the samples is not very significant, what proves the preservation of the crystalline, zeolitic character in the case of micro-mesoporous sample. On the other side generation of mesoporosity by mesotempate-free method strongly influenced the acidic properties of H-Beta/meso. Temperature-programmed desorption of ammonia (NH_3-TPD) was used to evaluate the nature of acid sites (concentration, strength) in H-Beta/meso. Both NH_3 desorption profiles of conventional Beta zeolite and the micro-mesoporous sample (shown in Fig. 2B) consist of two maxima, which are possible associated with the presence of weaker (max. at about 200°C) and stronger (max. about 350-400°C) acid sites. Basing on the literature the first maximum could be attributed to NH_3 bonded to silanol groups, while the second one to ammonia interacting with framework Al [27]. The intensity of ammonia desorption profile significantly decreased for the modified micro-mesoporous sample what was reflected in the changes in total concentration of acid sites (determined with the assumption that one NH_3 molecule adsorbs on one acid site), which was about twice smaller than in the case of conventional Beta zeolite. The changes observed in surface acidity

are also reflected in the Si/Al ratio of the samples measured by atomic absorption spectroscopy (Tab. 2). The micro-mesoporous sample Beta is characterised by the Si/Al ratio more than two times smaller than conventional microporous Beta. Both NH_3-TPD and AAS techniques proved that the applied method of mesoporosity generation by acidification of the zeolite nanoseeds slurry disturbs zeolite crystallization and affects the concentration of acid sites in the final catalyst.

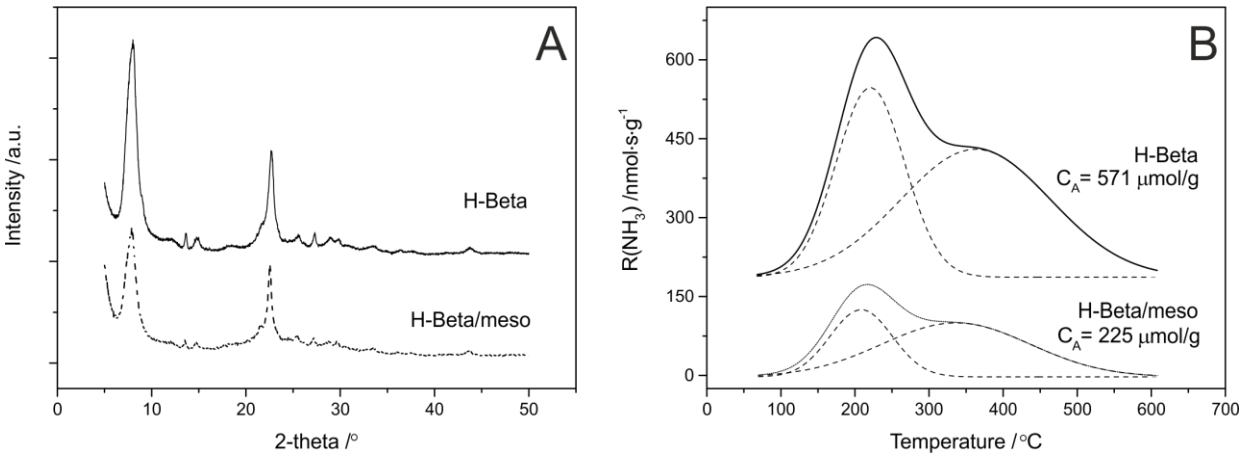

Fig. 2. XRD profiles (A) and NH_3-TPD profiles (B) of the parent H-Beta and H-Beta/meso samples

Summarizing, the zeolitic supports H-Beta and H-Beta/meso modified with Fe_xCr_y oligocations differ with respect to textural properties, crystallinity and acidity. It was found that the micro-mesoporous sample possess high external surface area and volume of mesopores, which were created in a favour of loose in microporosity, crystallinity and acidity of the sample.

Tab. 2. The Si/Al ratio and Fe and Cr content in the samples determined by AAS

Sample code	Si/Al	Fe [%wt]	Cr [%wt]	Fe [%mol]	Cr [%mol]	Fe+Cr [%mol]
H-Beta	16	---	---	---	---	
H-Beta/meso	27	---	---	---	---	
Fe3-Beta	15	2.9	---	1.5		1.5
Fe3-Beta/meso	28	3.7	---	1.9		1.9
Fe2Cr-Beta	15	2.3	0.4	1.2	0.2	1.4
Fe2Cr-Beta/meso	27	2.8	0.6	1.5	0.3	1.8
FeCr2-Beta	15	1.0	0.5	0.5	0.3	0.8
FeCr2-Beta/meso	27	1.0	0.9	0.5	0.5	1.0
Cr3-Beta	17	---	0.2		0.1	0.1
Cr3-Beta/meso	30	---	0.4		0.2	0.2
Fe-Beta	16	0.9	---	0.5		0.5
Fe-Beta/meso	29	0.7	---	0.4		0.4

3.2. Samples modified with Fe_xCr_y oligocations

Zeolitic supports, H-Beta and H-Beta/meso, described above were modified with Fe_xCr_y oligocations. In order to verify the proper structure of synthesized oligocations IR-DRIFT spectroscopy was used. The spectra of trinuclear acetate complexes reveal four characteristic bands related to symmetric and asymmetric vibrations of COO anions [19, 28]. The bands located at about 1600 and 1450 cm^{-1} are related to bridging acetate groups, while two others (at about 1690 and 1290 cm^{-1}) correspond to monodentate acetate groups [19, 28]. The examples of the spectra recorded for oxo-centred acetate complexes $[Cr_{3-x}Fe_xO(OAc)_6 \cdot AcOH \cdot 2H_2O]NO_3$ (where x = 1 or 2) are shown in Figs. 3A and 3B. Based on the recorded spectra it could be concluded that the structure of synthesized acetate complexes is similar to the structure of such oligocationic species reported previously in the literature [19, 28].

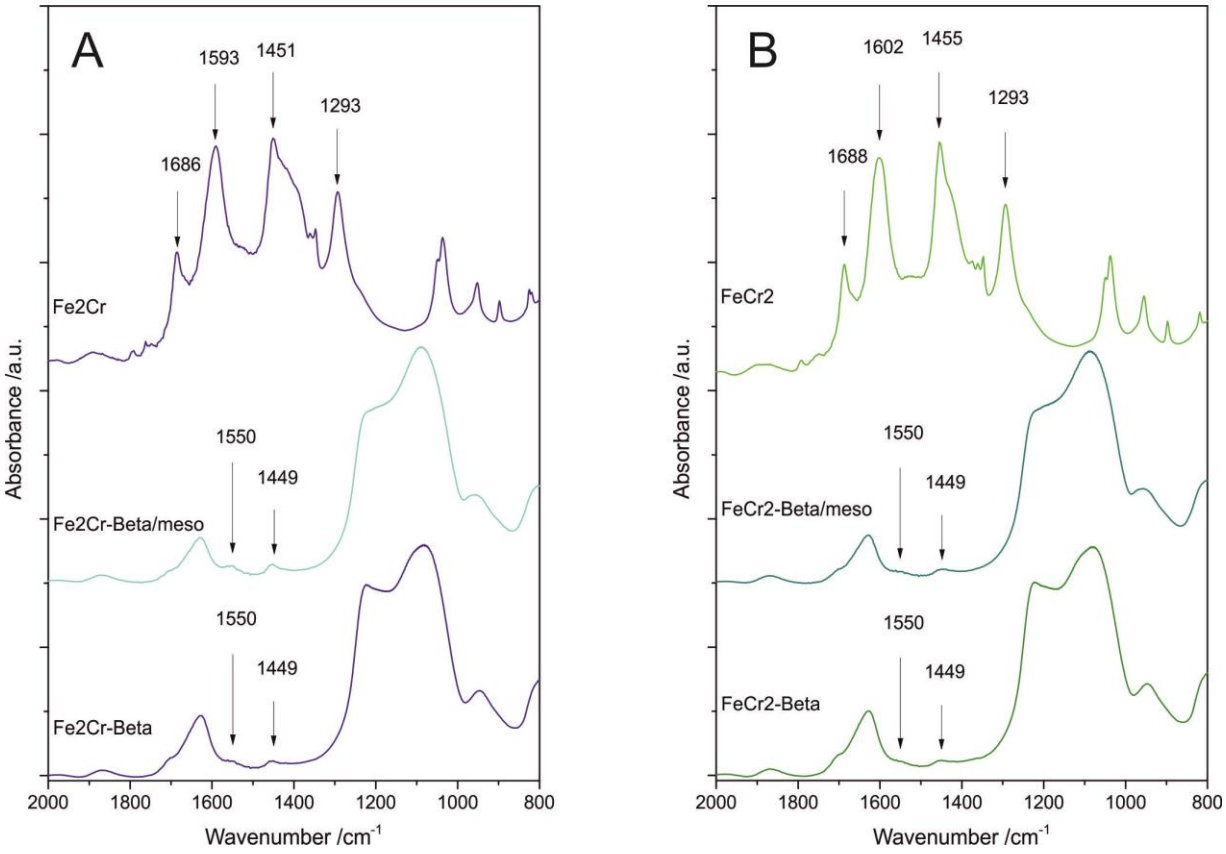

Fig. 3. IR-DRIFT spectra of Fe2Cr (A) and FeCr2 (B) oligocations and zeolitic supports H-Beta and H-Beta/meso modified with their use

The spectra of the microporous and micro-mesoporous Beta zeolites modified with bimetallic salts (Figs. 3A and 3B), recorded after their washing and drying, exhibit in both cases two weak absorption bands located at 1550 and 1449 cm^{-1}, which are characteristic of COO vibrations. It should be noted that the former band is shifted from 1600 cm^{-1} to 1550 cm^{-1} what indicates the changes in the transition metal-acetyl configuration during the ion-exchange process [19, 28]. The lack of COO vibrations at higher wavenumbers, connected with the presence of non-exchanged oligocationic species, confirms high efficiency of the washing step [19, 28].

Dinitrogen sorption isotherms obtained for the samples modified with Fe_xCr_y oligocations (Fig. 4A) do not differ significantly from the isotherms recorded for the supports –

conventional and micro-mesoporous Beta zeolites (Fig. 1A). Only in the case of Fe3-Beta/meso smaller amount of adsorbed N_2 volume was observed. Greater differences are visible in the pore size distributions (Fig. 4B). After modification of the micro-mesoporous samples with oligocations the pore sizes distribution was shifted into lower values and became more jagged. This phenomenon is especially visible in the case of the samples modified with Fe3 oligocations and can be connected with the mesopore blocking. Textural parameters of the zeolitic supports (Tab. 1) changed slightly after their modification with transition metals. The BET surface area and volume of micropores decreased for all the samples, what can be connected with the blocking of micro and mesopores by metal oxide aggregates. The external surface area and mesopore volume in the case of majority of the samples slightly increased, what is possible related to reorganization of the inter-particle mesoporosity during the subsequent hydrothermal treatment or to the surface development in a favour of metal aggregates deposition on the surface.

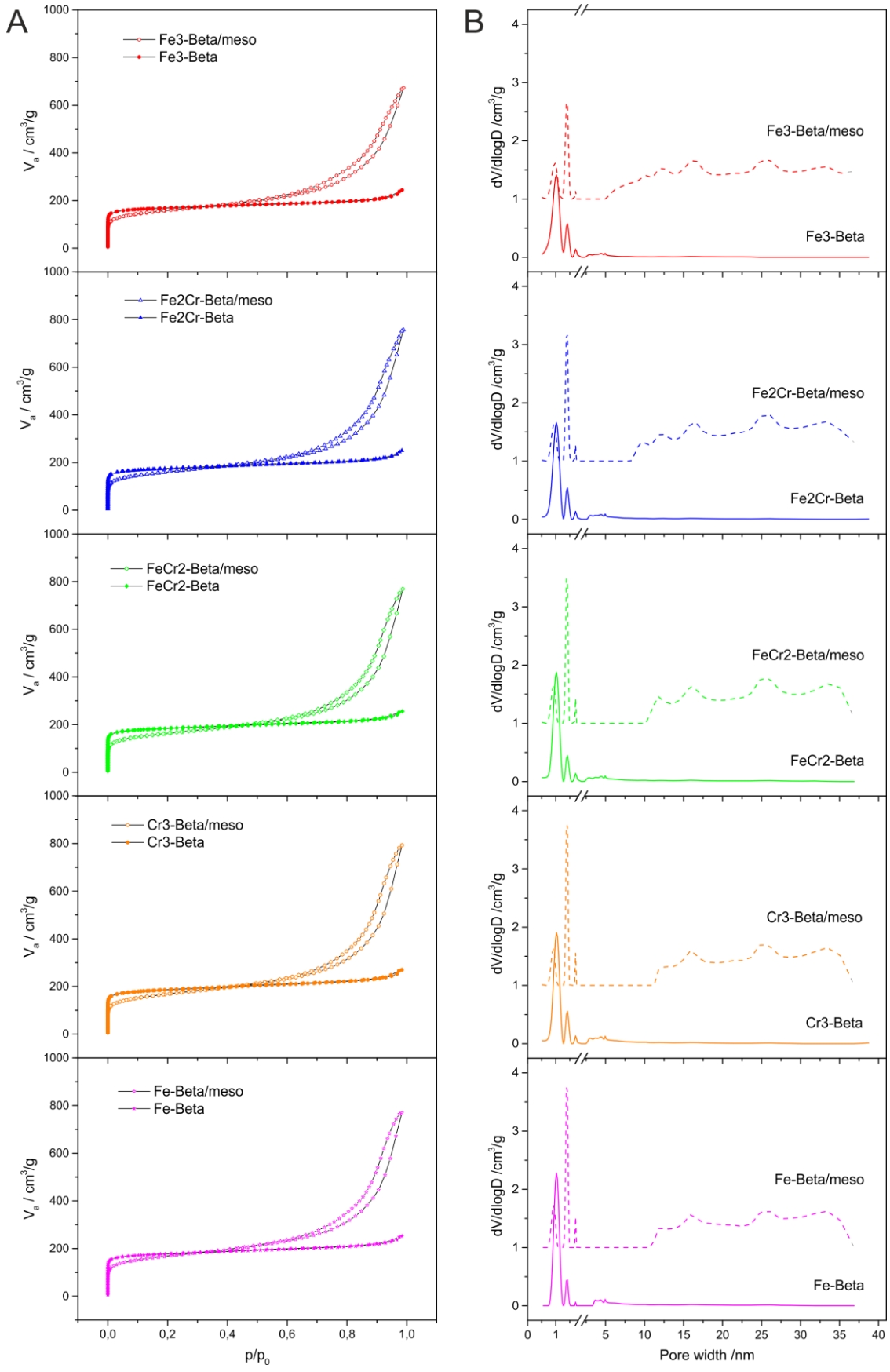

Fig. 4. Dinitrogen adsorption-desorption isotherms (A) and pore size distribution (B) of the samples modified with Fe_xCr_y oligocation

The Si/Al ratios of the samples, presented in Tab. 2, did not change significantly after their modification with transition metals. More interesting phenomenon was observed for metal contents (Tab. 2). In the case of the samples modified with oligocations the higher amount of metals was introduced into the Beta/meso series. This effect could be explained by the more open and loose porous structure (increased mesoporosity) and therefore better accessibility of ion-exchange positions. Only in the case of the Fe-Beta and Fe-Beta/meso samples, modified by ion-exchange method with an aqueous solution of $FeSO_4$, a slightly higher amount of Fe was introduced to conventional Beta zeolite. It seems that in the case of isolated cations, the modification of the porous structure had a smaller impact on the amount of introduced metal species than the surface acidity of the samples (straight connection with the number of ion-exchange positions), which was smaller in the case of Beta/meso series. Comparing the samples modified with iron in the form of oligocations (Fe3-Beta, Fe3-Beta/meso) and solution of $FeSO_4$ (Fe-Beta, Fe-Beta/meso) larger amount of Fe was introduced by the former method. In the case of conventional Beta zeolite exactly 3 times more iron was introduced by deposition oligocations in comparison to ion-exchange with a solution of $FeSO_4$. Thus it could be concluded that all ion-exchange positions accessible for monomeric cations were also accessible for oligocations.

The analysis of the UV-vis-DR spectra of these samples (Fig. 5) gives more information about the chemical nature of deposited transition metal species. Small absorption band observed below 250 nm is possibly related to the presence of Fe^{3+} cations in tetrahedral coordination, however it is also possible that this signal is associated with charge transfer (CT) in the zeolite framework ($O^{2-} \rightarrow Al^{3+}$) [29]. The following bands with maxima at about 250-300 and 300-400 nm can be connected with the presence of monomeric iron cations in octahedral coordination and Fe_xO_y oligomeric species, respectively, while the band located

above 400 nm Fe_2O_3 is related to oxide particles [30, 31]. In the case of the Fe-Beta and Fe-Beta/meso samples iron was introduced mainly in the form of monomeric Fe^{+3} cations, while in the case of the samples modified by Fe3 oligocations the contribution of oligomeric species is significantly larger (what was expected by the method used). For the samples modified with oligocations, higher content of the aggregated iron oxide species was observed in the case of conventional Beta zeolite. This phenomenon can be connected with the mesoporosity generation (more developed, open structure), which in the case of Fe3-Beta/meso enabled better metal dispersion on the sample surface. Reverse effect, higher metal aggregation for Fe-Beta/meso, could be connected with the lower acidity of the micro-mesoporous sample, what forced slight metal aggregation. However, it should be stressed that this effect was not significant and monomeric Fe^{3+} species were the main form of iron in the samples modified with a $FeSO_4$ solution.

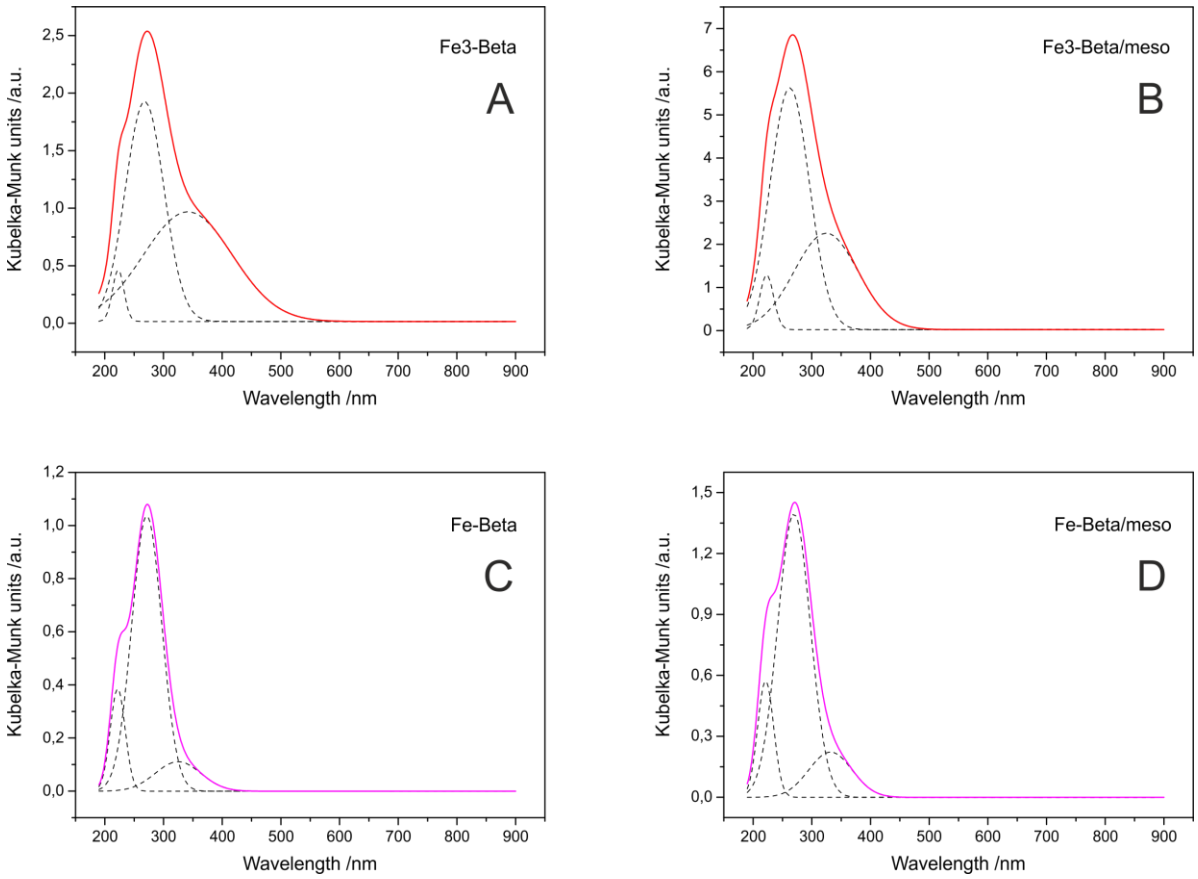

Fig. 5. UV-vis-DR spectra of the Beta and Beta/meso samples modified with iron using oligocations (A, B) and $FeSO_4$ solution (C, D)

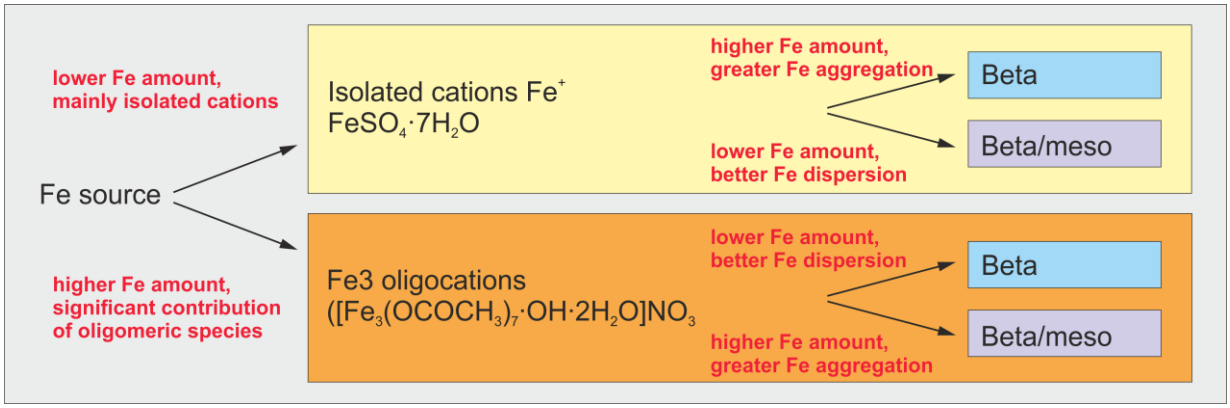

Scheme.1. Scheme presenting iron content and aggregation level, depending on the on the used Fe source and catalyst support (Beta or Beta/meso)

Analysing correlation between iron content and its aggregation in the samples and the used iron source ($FeSO_4$ solution or Fe3 oligocations) and porous nature of the support (Beta or Beta/meso) (scheme 1), it can be concluded that higher amount of iron can be introduced with the use of oligocations as iron species precursor. Moreover, a significant contribution of small oligomeric species increased for micro-mesoporous zeolite, for which a more open structure limits the aggregation of highly dispersed species into bulky iron oxide. It is worth to emphasize, that conventional methods, which enable introduction of higher metal contents into zeolites, such as impregnation, do not lead to uniform, high dispersion of metal on the surface.

In the case of chromium modified samples (Fig. 6A and 6B) despite the band below 250 nm (from the zeolite structure) three bands with maxima located at about 250, 350 and 450 nm can be distinguished. These peaks are connected with the presence of tetrahedrally coordinated Cr^{6+} in small mono- or polychromate species [32-34]. Any absorption above 600 nm, related to the presence of Cr^{3+} in ion-exchange positions (complete oxidation $Cr^{3+} \rightarrow Cr^{6+}$ during calcination) or in the form of Cr_2O_3 or Cr_xO_y clusters (high aggregation on the surface) was observed [32-34].

Analysis of the spectra obtained for the samples modified with Fe2Cr (Fig. 6C and 6D) and Fe2Cr oligocations (Fig. 6E and 6F) is not apparent because of the superposition of the absorption bands from iron and chromium. However, the shapes of the mixed metal oligocations are similar to the spectra of iron modified samples (Fig. 5) with the superposition of chromium adsorption, rising the spectra intensity at about 350-500 nm. The same as in the case of Fe3 series (Fig. 5A and B) modification of H-Beta zeolite with Cr3, FeCr2 and Fe2Cr oligocations (Fig. 6) resulted in slightly higher aggregated species in comparison to a Beta/meso series.

The intensity of the UV-vis adsorption bands does not give the information about the content the of particular metal form (different extinction coefficients), however analysing the Fe and Cr contents in the samples determined by AAS (Tab.2), iron was introduced in a significantly higher amounts in comparison to chromium. Despite the same modification procedure used, iron was introduced preferentially into the samples. Also in the case of mixed oligocations the molar ratio between Fe and Cr was not preserved. This result suggest that in the used oligocations solutions (under the applied ion-exchange conditions) some part of metals was present in the form of isolated cations. In case of Cr^{6+}, potentially present in the solution of oligocations, one mole of chromium cations would compensate 6 ion-exchange positions, what could be a reason of smaller chromium content in the samples. However this phenomenon is still not clear.

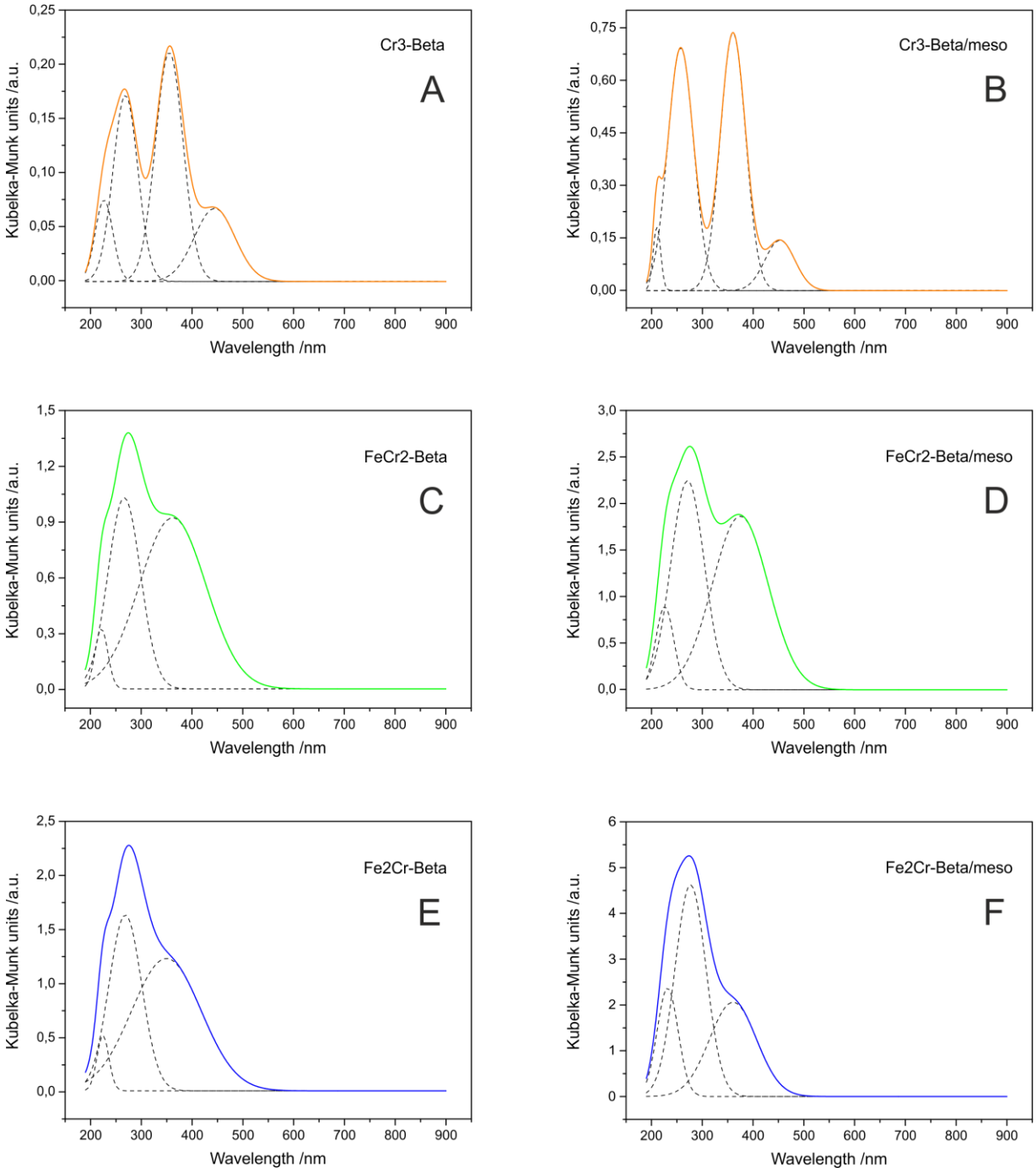

Fig. 6. UV-vis-DR spectra of the Beta and Beta/meso samples modified with chromium (A, B) and iron-chromium (C-F) oligocations

The red-ox properties of the samples were analysed by temperature programmed reduction with hydrogen (H_2-TPR) (Fig. 7). In the case of Fe3-Beta and Fe3-Beta/meso one broad reduction peak at about 300-500°C was observed. This reduction peak can be assigned to the reduction of $Fe^{3+} \rightarrow Fe^{2+}$ (monomeric or oligomeric). The lack of hydrogen consumption

above 500°C proves that FeO or Fe_3O_4 oxide species were not formed in the samples [35-37]. Also in the case of the samples modified with Cr3 oligocations one broad reduction peak was detected. It could be related to the reduction of $Cr^{6+} \rightarrow Cr^{3+}$ (at about 350°C), $Cr^{3+} \rightarrow Cr^{0}$ from monomeric cations (at about 400°C) and more aggregated oxo-species (at about 450°C) [32, 38, 39]. In the case of micro-mesoporous sample the reduction peak is shifted into higher temperatures, what can be connected with a better dispersion of chromium species. According to Ayari et. al. [38] clustered Cr species are more easily reduced in the comparison to more dispersed once. The reduction profiles of the samples modified with Fe2Cr and FeCr2 oligocations are a superposition of the iron and chromium reduction profiles and therefore the detailed relation of the specific subbands to the reduction of transition various possible metal species is very difficult or even impossible. However, it is very important to notice that by the modification of the samples with bimetallic oligocations the reducibility properties of the samples were changed. The shift into lower temperatures of the reduction peaks can be connected with the enhanced red-ox properties of the samples, what is very important in the case of the examined catalytic reaction, NH_3-SCO process.

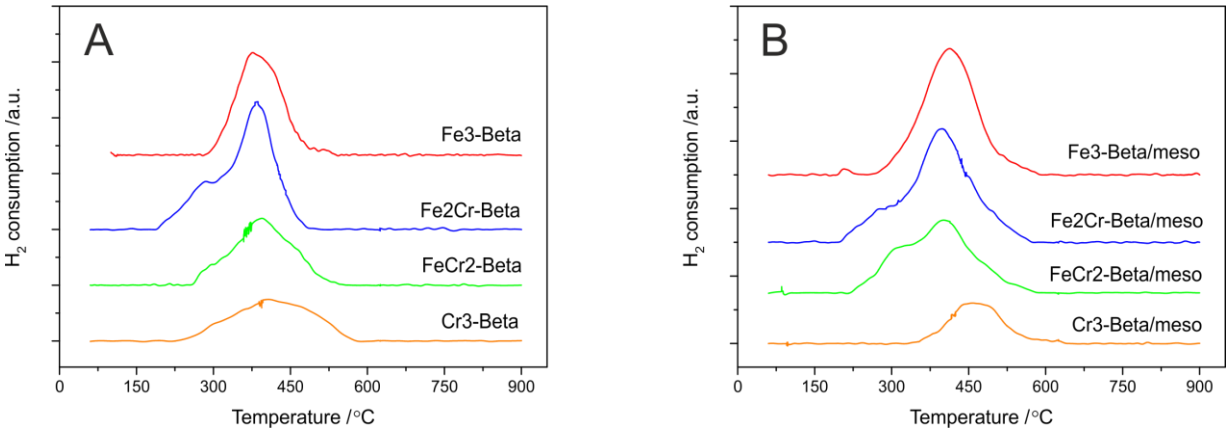

Fig. 7. H_2-TPR profiles of the Beta (A) and Beta/meso (B) samples modified with Fe_xCr_y oligocations

3.3. Catalytic study

Catalytic activity of the prepared series of the samples is presented in Fig.8. Modification of H-Beta and H-Beta meso (Fig. 8A) with iron and chromium species significantly increased their activity in the process of selective ammonia oxidation, what proves an important role of red-ox active sites in the mechanism of this reaction. Comparing the samples modified with iron oligocations (Fig. 8B) and iron isolated cations (Fig. 8F) the higher catalytic activity was obtained over Fe3-Beta and Fe3-Beta/meso. This difference in the catalytic activity can be connected with a significantly higher Fe content in the samples modified with Fe3 oligocations solution. What means that the use of iron oligocations for the modification of zeolites, has a positive impact on the samples activity in selective ammonia oxidation. It is important to notice that introduction of higher metal content in comparison to standard ion-exchange did not resulted in the formation of Fe bulky species that can block the pore system and deactivate the catalyst.

Among the samples modified with Fe_xCr_y oligocations very high activity presented the catalysts containing chromium. Even the samples modified with Cr3 oligocations, despite a very low content of chromium, show 100% NH_3 conversion at relatively broad temperature range of 450-600°C (Fig. 8E). The results clearly shows that for the high catalytic activity in this reaction mainly chromium species are responsible, however it also seems that iron presence enhances the reaction selectivity to dinitrogen. It can be concluded that the best results with respect to high catalytic activity and very high selectivity to N_2 (>95%) were obtained for the samples modified with Fe2Cr oligocations (Fe2Cr-Beta and Fe2Cr-Beta/meso, Fig. 8C), what proves a positive effect of the bimetallic systems.

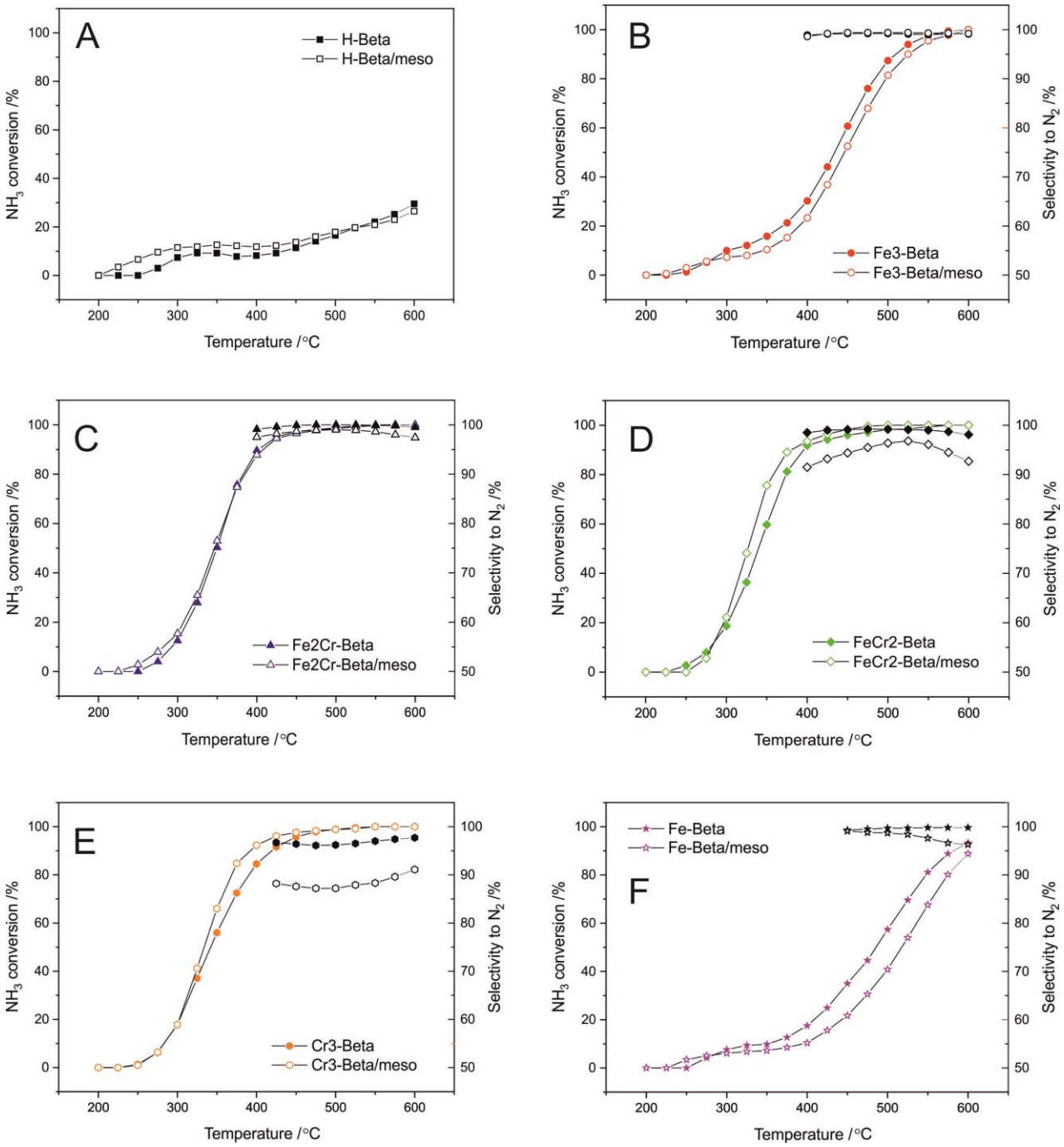

Fig. 8. Temperature dependence of NH_3 conversion and N_2 selectivity for the samples H-Beta and H-Beta/meso (A) modified with Fe_xCr_y oligocations (B-E) and $FeSO_4$ solution (F). Conditions: 5000 ppm NH_3, 25000 ppm O_2; He as balancing gas; total flow rate - 40 ml/min; weight of catalyst - 0.1 g

The catalytic activity of the samples can be also compared basing on the T_{50} (temperature needed to obtain 50% conversion), shown in Fig. 9. The lowest T_{50} (the highest activity) was obtained for the samples modified with bimetallic Fe2Cr, FeCr2 and purely chromium (Cr3)

oligocations. The catalytic activity of the Beta/meso samples modified with chromium was higher in comparison to Beta series containing this metal species. In the case of the samples modified only with iron (independently from iron precursor used) higher activity was obtained for the H-Beta series. These results suggest that in the case of iron doped samples more aggregated species are more active in NH_3-SCO, while in the case of chromium isolated cations or small oligomers.

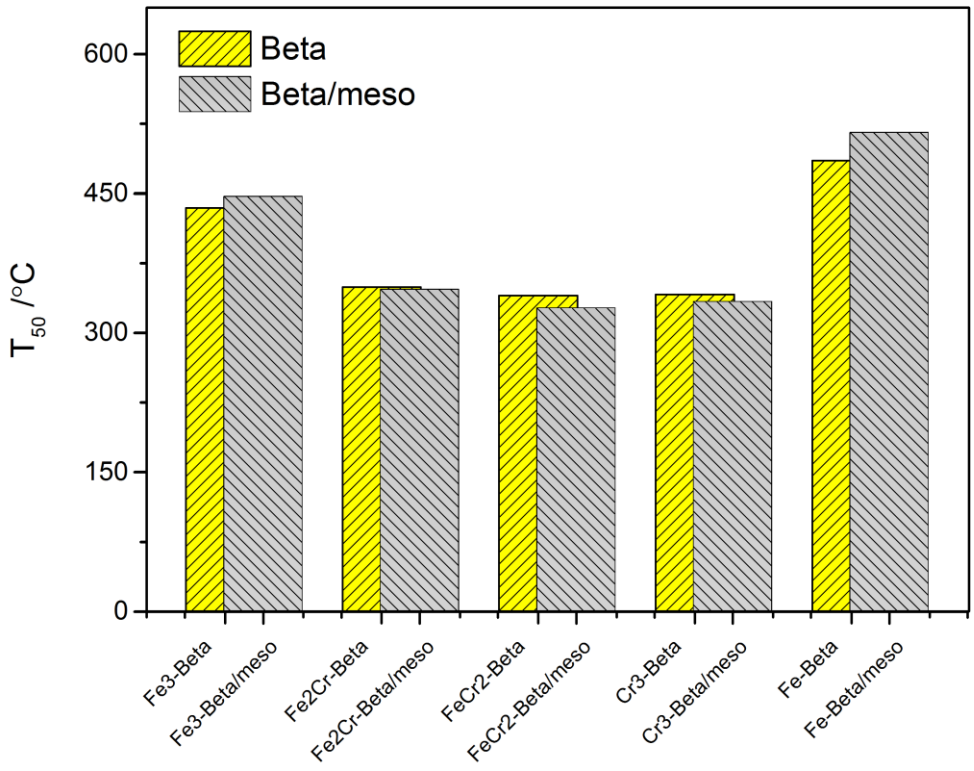

Fig. 9. Temperature of 50% conversion of the samples modified with Fe_xCr_y oligocations and $FeSO_4$ solution.

It is very important to emphasise that the comparison of the catalytic activity of the samples differing in the metal content make sense from the point of view of the synthesis concept. The proposed modification method of the zeolitic systems with oligocations enables introduction of higher metal contents (with the same modification procedure as in the case of a $FeSO_4$ solution) what results in a higher catalytic activity per gram of the obtained catalysts.

However, the research have to be continued and mainly focused on the recognition of the mechanism of particular oligocations deposition and optimisation of the multimetalic oligocations composition for the formulation of more effective catalysts for the process of selective oxidation of ammonia to dinitrogen.

4. Conclusions

In the presented studies mesoporous Beta zeolite was obtained by mesotemplate-free method. The H-Beta/meso sample was characterized by significantly higher external surface area and mesopores volume in comparison to conventional, microporous H-Beta zeolite. Development of mesoporosity was connected with a decrease in microporosity, crystallinity and acidity, however the zeolitic character of the sample was still preserved. Modification of H-Beta with Fe3 oligocations resulted in an introduction of three times higher amount of iron in comparison to the sample modified with a solution of $FeSO_4$. Depending on the iron source used different amounts and forms of Fe were introduced into H-Beta/meso. In the case of Fe3 oligocations the more opened structure of the mesoporous sample enabled introduction of larger amount of iron in the more aggregated forms. On the other side, in the case of the zeolite support modification with a solution of $FeSO_4$ the lower content of highly dispersed iron species was deposited. In the case of the Beta/meso samples modified with Fe_xCr_y better dispersion of smaller particles with enhanced reducibility was found.

Despite significantly smaller amount of Cr in the samples the catalysts containing chromium showed higher activity in the NH_3-SCO process in comparison to iron modified ones. However, it seems that the presence of iron also plays an important role, especially in term of selectivity, directing the reaction into dinitrogen production. In the case of the samples modified with Fe2Cr, FeCr2 and Cr3 oligocations slightly higher activity was observed for

the Beta/meso samples, what can be connected with better dispersion and enhanced reducibility properties of the particles introduced into this series of the catalysts.

Acknowledgements

This work was carried out in the frame of project no. 0670/IP3/2016/74 from the Polish Ministry of Science and Higher Education in the years 2016/2019 and in the frame of project no. 2012/05/B/ST5/00269 from the National Science Centre (Poland).

References

[1] L. Chmielarz, M. Jabłońska, *RSC Advances* 5 (2015) 43408-43431.

[2] M. Jabłońska, R. Palkovits, *Applied Catalysis B: Environmental* 181 (2016) 332-351.

[3] G. Qi, J.E. Gatt, R.T. Yang, *Journal of Catalysis* 226 (2004) 120-128.

[4] A. Akah, C. Cundy, A. Garforth, *Applied Catalysis B: Environmental* 59 (2005) 221-226.

[5] P. Li, R. Zhang, N. Liu, S. Royer, *Applied Catalysis B: Environmental* 203 (2017) 174-188.

[6] L. Chmielarz, P. Kuśtrowski, M. Drozdek, R. Dziembaj, P. Cool, E.F. Vansant, *Catalysis Today* 114 (2006) 319-325.

[7] L. Chmielarz, A. Węgrzyn, M. Wojciechowska, S. Witkowski, M. Michalik, *Catalysis Letters* 141 (2011) 1345-1354.

[8] L. Chmielarz, M. Jabłońska, A. Strumiński, Z. Piwowarska, A. Węgrzyn, S. Witkowski, M. Michalik, *Applied Catalysis B: Environmental* 130-131 (2013) 152-162.

[9] A. Kowalczyk, A. Borcuch, M. Michalik, M. Rutkowska, B. Gil, Z. Sojka, P. Indyka, L. Chmielarz, *Microporous and Mesoporous Materials* 240 (2017) 9-21.

[10] M. Jabłońska, A. Król, E. Kukulska-Zając, K. Tarach, L. Chmielarz, K. Góra-Marek, *Journal of Catalysis* 316 (2014) 36-46.

[11] L. Chmielarz, P. Kuśtrowski, A. Rafalska-Łasocha, R. Dziembaj, *Applied Catalysis B: Environmental* 58 (2005) 235-244.

[12] M.S. Kim, D.W. Lee, S.H. Chung, Y.K. Hong, S.H. Lee, S.H. Oh, I.H. Cho, K.Y. Lee, *Journal of Hazardous Materials* 237-238 (2012) 153-160.

[13] M. Rutkowska, L. Chmielarz, D. Macina, Z. Piwowarska, B. Dudek, A. Adamski, S. Witkowski, Z. Sojka, L. Obalová, C.J. Van Oers, P. Cool, *Applied Catalysis B: Environmental* 146 (2014) 112-122.

[14] R.Q. Long, R.T. Yang, *Chemical Communications* 16 (2000) 1651-1652.

[15] N.N. Sazonova, A.V. Simakov, T.A. Nikoro, G.B. Barannik, V.F. Lyakhova, V.I. Zheivot, Z.R. Ismagilov, H. Veringa, *Reaction Kinetics and Catalysis Letters* 57 (1996) 71-79.

[16] T. Curtin, S. Lenihan, *Chemical Communications* 11 (2003) 1280-1281.

[17] S. Lenihan, T. Curtin, *Catalysis Today* 145 (2009) 85-89.

[18] A. Akah, C. Cundy, A. Garforth, *Applied Catalysis B: Environmental* 59 (2005) 221-226.

[19] D. Macina, A. Opioła, M. Rutkowska, S. Basąg, Z. Piwowarska, M. Michalik, L. Chmielarz, *Materials Chemistry and Physics* 187 (2017) 60-71.

[20] M. Rutkowska, Z. Piwowarska, E. Micek, L. Chmielarz, *Microporous and Mesoporous Materials* 209 (2015) 54-65.

[21] M. Rutkowska, M. Duda, A. Kowalczyk, L. Chmielarz, *Comptes Rendus Chimie* 20 (2017) 850-859.

[22] M. Rutkowska, I. Pacia, S. Basąg, A. Kowalczyk, Z. Piwowarska, M. Duda, K.A. Tarach, K. Góra-Marek, M. Michalik, U. Díaz, L. Chmielarz, *Microporous and Mesoporous Materials* 246 (2017) 193-206.

[23] M. Rutkowska, U. Díaz, A.E. Palomares, L. Chmielarz, *Applied Catalysis B: Environmental* 168 (2015) 531-539.

[24] K. Góra-Marek, K. Brylewska, K.A. Tarach, M. Rutkowska, M. Jabłońska M. Choi, L. Chmielarz, *Applied Catalysis B: Environmental* 179 (2015) 589-598.

[25] J. Rouquerol, P. Llewellyn, F. Rouquerol, *Studies in Surface Science and Catalysis* 160 (2007) 49-56.

[26] M. Thommes, K. Kaneko, A.V. Neimark, J.P. Olivier, F. Rodriguez-Reinoso, J. Rouquerol, K.S.W. Sing, *Pure Applied Chemistry* 87(9-10) (2015) 1051-1069.

[27] Q. Shen, L. Li, C. He, X. Zhang, Z. Hao, Z. Xu, *Asia-Pacific Journal of Chemical Engineering* 7 (2012) 502-509.

[28] N. Maes, E.F. Vansant, *Microporous and Mesoporous Materials*, 4 (1995) 43-51.

[29] E.D. Garbowski, C. Mirodatos, *Journal of Physical Chemistry* 86 (1982) 97-102.

[30] A. Wang, Y. Wang, E.D. Walter, R.K. Kukkadapu, Y. Guo, G. Lu, R.S. Weber, Y. Wang, C.H.F. Peden, F. Gao, *Journal of Catalysis*, 358 (2018) 199-210.

[31] Y. Xia, W. Zhan, Y. Guo, Y. Guo, G. Lu, *Chinese Journal of Catalysis*, 37 (2016) 2069-2078.

[32] Y. Cheng, F. Zhang, Y. Zhang, C. Miao, W. Hua, Y. Yue, Z. Gao, *Chinese Journal of Catalysis*, 36 (2015) 1242-1248.

[33] J. Wang, J. Xie, Y. Zhou, J. Wang, *Microporous and Mesoporous Materials*, 171 (2013) 87-93.

[34] D. Esquivel, A.J. Cruz-Cabeza, C. Jiménez-Sanchidrián, F.J. Romero-Salguero, *Microporous and Mesoporous Materials*, 179 (2013) 30-39.

[35] S.S. Reddy Putluru, A. Degn Jensen, A. Riisager, R. Fehrmann, *Topics in Catalysis*, 54 (2011) 1286-1292.

[36] L. Li, Q. Shen, J. Li, Z. Hao, Z. Ping Xu, G.Q.M. Lu, *Applied Catalysis A: General*, 344 (2008) 131-141.

[37] A. Guzmán-Vargas, G. Delahay, B. Coq, *Applied Catalysis B: Environmental*, 42 (2003) 369-379.

[38] F. Ayari, M. Mhamdi, T. Hammedi, J. Álvarez-Rodríguez, A.R. Guerrero-Ruiz, G. Delahay, A. Ghorbel, *Applied Catalysis A: General*, 439-440 (2012) 88-100.

[39] P. Liu, X. Zhang, Y. Yao, J. Wang, *Applied Catalysis A: General*, 371 (2009) 142-147.